

## Research Article

# Optical and Electrical Studies of Polyaniline/ZnO Nanocomposite

Manawwer Alam,<sup>1</sup> Naser M. Alandis,<sup>2</sup> Anees A. Ansari,<sup>3</sup> and Mohammed Rafi Shaik<sup>2</sup>

<sup>1</sup> Research Center, College of Science, King Saud University, P.O. Box 2455, Riyadh 11451, Saudi Arabia

<sup>2</sup> Department of Chemistry, College of Science, King Saud University, P.O. Box 2455, Riyadh 11451, Saudi Arabia

<sup>3</sup> King Abdullah Institute for Nanotechnology, King Saud University, P.O. Box 2455, Riyadh 11451, Saudi Arabia

Correspondence should be addressed to Manawwer Alam; malamiitd@gmail.com

Received 22 September 2013; Accepted 9 December 2013

Academic Editor: John Zhanhu Guo

Copyright © 2013 Manawwer Alam et al. This is an open access article distributed under the Creative Commons Attribution License, which permits unrestricted use, distribution, and reproduction in any medium, provided the original work is properly cited.

Polyaniline (Pani)/ZnO nanocomposite with diameter 40–50 nm was successfully fabricated by coprecipitation method of ZnO via *in situ* polymerization of Pani. X-ray diffraction (XRD), high resolution transmission electron microscopy (HRTEM), fourier transformation infrared (FT-IR), UV-Vis absorption spectra, thermogravimetric analysis (TGA), and electrical properties were studied. HRTEM studies showed that the prepared ZnO nanoparticles were uniformly dispersed and highly stabilized throughout the polymer chain and formed uniform metal oxide-conducting polymer nanocomposite material. UV-Vis spectra of Pani/ZnO nanocomposite were studied to investigate the optical behavior after doping the ZnO nanoparticle into the polymer matrix. The inclusion of ZnO nanoparticle gives rise to the red shift of  $\pi-\pi^*$  transition of Pani. The nanocomposite was found to be thermally stable upto 130°C and showed conductivity value of  $3.0 \times 10^{-2} \text{ Scm}^{-1}$ .

## 1. Introduction

Pani, a conducting polymer, has increasing scientific and technological interests in the synthesis of a broad variety of promising materials due to its unique electrical and optical properties [1, 2]. Pani is widely used in the area of electrochemical materials, light-emitting diodes, biosensors, chemical sensors, and battery electrodes [3–5]. Recently, extensive research has been focused on the synthesis and potential applications in electronic devices to enhance the electrical properties of Pani [6].

Numerous efforts have been made to successfully prepare nanocomposites by chemical and electrochemical preparation methods using nanostructured metal oxides namely  $\text{TiO}_2$ ,  $\text{SnO}_2$ ,  $\text{SiO}_2$ ,  $\text{CeO}_2$ , and  $\text{Fe}_2\text{O}_3$  due to their unique electrocatalytic, piezoelectric, and photonic properties and tunable size that make them suitable for solar cell applications [7–11]. These nanocomposites show quite different properties than the individual materials. Nanostructured zinc oxide (ZnO) has unique properties like high isoelectric point,

transparent n-type semiconductor with direct wide band gap (3.37 eV), biocompatibility, nontoxicity, high chemical stability, high electron transfer capability, and others [12–18] with various potential applications such as in gas sensor, biological sensor, ultraviolet light emitting diodes, dye sensitized solar cells, photocatalysis, ceramics, cosmetics, and paint industry [19–31].

In the present work, we report the synthesis of ZnO nanoparticle and ZnO nanoparticle doped in Pani using coprecipitation method and observed the optical, electrical, and thermal properties of Pani/ZnO nanocomposite. The prepared Pani/ZnO nanocomposite was characterized by FT-IR, XRD, UV-Vis, TGA, and conductivity studies.

## 2. Experimental

**2.1. Materials.** Aniline and Zinc acetate (BDH chemical Poole, England) were distilled under reduced pressure before use. Ammonium peroxodisulfate (APS), Ammonium hydroxide (Merck, India), and other chemicals used were of

analytical grade. The deionized water obtained from Millipore system was used for the synthesis.

**2.2. Synthesis of Pani.** 20 mL double distilled aniline with 1 M HCl in 250 mL round bottom flask at 27°C was stirred for 30 minutes and subsequently 125 mL of 1 M APS solution was added dropwise. After the addition of APS, stirring of the reaction mixture was continuously carried out up to 4 hours, resulting in thick green solution kept for 24 hours. The precipitate was washed with 1 M HCl and tetrahydrofuran to remove oligomers; the solution turned colourless and it was then dried in vacuum oven at 60°C for 24 hours to obtain green colored Pani (emeraldine) [8].

**2.3. Synthesis of Pani/ZnO Nanocomposite.** 1.0 g Zn (CH<sub>3</sub>COO)<sub>2</sub> · 2H<sub>2</sub>O was dissolved in 50 mL distilled water. 5 mL ammonium hydroxide solution (1 M) was added dropwise and the contents were mixed under vigorous stirring at 27°C for 6 hours. On addition of ammonia solution (pH 10), a white milky precipitate was obtained, and then subsequently Pani (10 wt%) was added. The precipitate was centrifuged and washed several times with distilled water to remove any residual reactants (NH<sup>+</sup><sub>4</sub>, Cl<sup>-</sup>) (neutral pH) and dried in oven at 80°C.

### 3. Characterization

Nanocomposites characterization by Powder XRD was carried out on a Rigaku Miniflex X-ray diffractometer (Japan) with Cu K $\alpha$  ( $\lambda$  = 1.5406) radiation. The patterns were recorded in the 2 $\theta$  range from 10° to 70° with scanning rate of 0.05/s. HRTEM was performed on JEM-2100F model of JEOL at 120 kV accelerated voltage in order to observe the size of ZnO nanoparticle in Pani. FT-IR spectra of the nanocomposite was recorded on a Nicolet iS 10, Thermo Scientific IR spectrometer (USA) in KBr disc at room temperature. The UV-Vis absorption spectra of the samples in methanol were recorded in the range of 200–400 nm by PerkinElmer LAMBDA 35 UV-Vis spectrophotometer (USA). Pellets of Pani/ZnO nanocomposite were made with compression molding machine with hydraulic pressure. High pressure was applied (10 tons) to the sample to obtain hard round pellet (diameter 18 mm, thickness 2 mm); these pellets were used to measure the conductivity with four probe technique at room temperature. The current voltage characteristics were studied with Kiethly 2400 source meter (USA). Voltage was applied to measure current through the sample. Thermogravimetric analysis (TGA) was performed with TGA1 (Mettler Toledo AG, Analytical CH-8603, Schwerzenbach, Switzerland) at 10°C/min in nitrogen atmosphere.

### 4. Results and Discussion

FT-IR spectra (Figure 1) of Pani and Pani/ZnO nanocomposite were taken to evaluate the interactions between Pani and ZnO nanoparticle. The characteristic peaks at 1562 cm<sup>-1</sup> and 1495 cm<sup>-1</sup> are due to the presence of quinonoid and benzenoid rings, respectively. The peaks at 1562 cm<sup>-1</sup> and

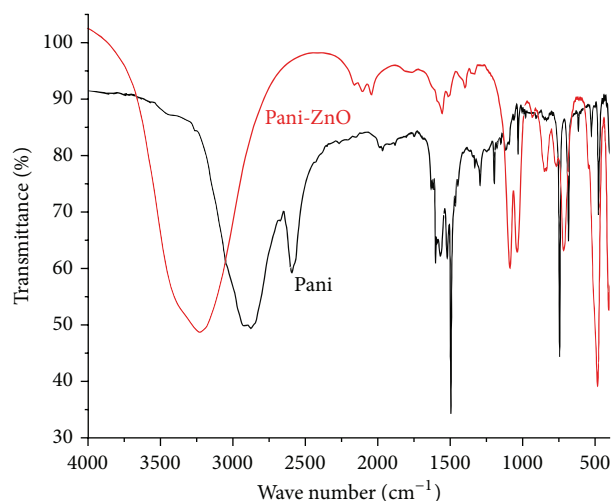


FIGURE 1: FT-IR spectra of Pani and Pani/ZnO nanocomposite.

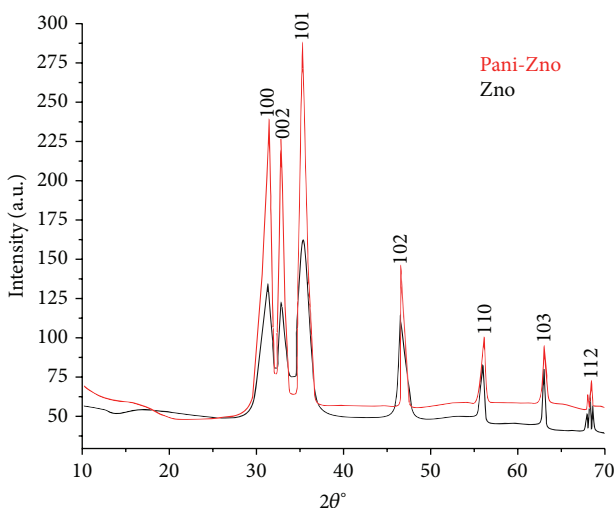


FIGURE 2: X-ray diffraction pattern of ZnO and Pani/ZnO nanocomposite.

1496 cm<sup>-1</sup> are assigned to C–C ring asymmetric and symmetric stretching vibrations. The peak at 2875 cm<sup>-1</sup> corresponds to C–H stretching. FT-IR spectra of Pani/ZnO nanocomposite in presence of metal oxide exhibit new absorption peaks distinctly at 3223 cm<sup>-1</sup>, 852 cm<sup>-1</sup>, 745 cm<sup>-1</sup>, and 477 cm<sup>-1</sup> assigned to the presence of metal oxide in the nanocomposite. The peak at 3223 cm<sup>-1</sup> can be attributed to N–H stretching and peak at 852 cm<sup>-1</sup>, 745 cm<sup>-1</sup>, and 477 cm<sup>-1</sup> correspond to Zn–OH, Zn–O–Zn bond, and free oxides.

The XRD patterns of pure ZnO and Pani/ZnO nanocomposite are shown in Figure 2. The XRD patterns indicate that the nanocomposite is well crystalline and reveals all diffraction peaks, which are perfectly similar to the literature (JCPDS no. 751526). The observed reflection planes resemble the tetragonal ZnO nanostructure; it can be seen that the reflections are markedly broadened, indicating crystalline size of ZnO nanoparticles of 40–50 nm by using Scherrer's

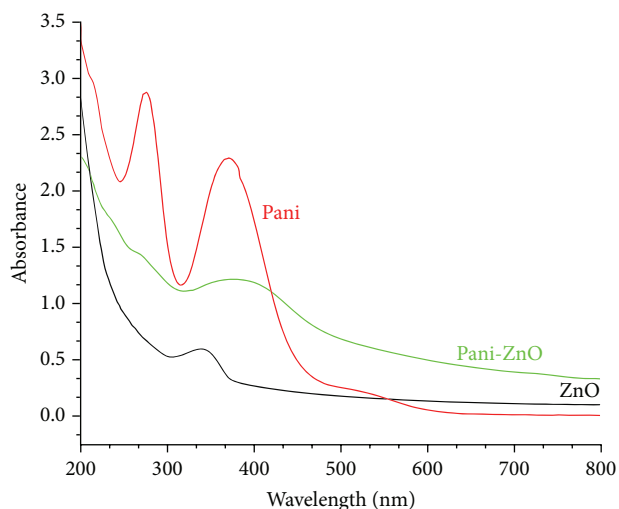


FIGURE 3: UV-Vis spectra of Pani, ZnO nanoparticle, and Pani/ZnO nanocomposite.

equation [29]. After addition of Pani in ZnO, nanoparticles were found crystallinity distributed in Pani/ZnO nanocomposites and similar observation also reported in the literature [29].

Figure 3 shows UV-Vis absorption spectra of the pure Pani, ZnO nanoparticle, and Pani/ZnO nanocomposite in aqueous solutions. It can be seen that ZnO nanoparticles showed strong absorption band in the UV region. Three characteristics absorption bands are shown in the spectrum of Pani at 275 nm, 366 nm, and 570 nm attributed to  $\pi$ - $\pi^*$  conjugated ring system, polaron  $\pi^*$ , and  $\pi$  polaron transitions, respectively. These results showed that Pani was completely converted from emeraldine salt to the emeraldine base form by the deprotonation of Pani with  $\text{NH}_4\text{OH}$ .

HRTEM micrographs (Figures 4(a) and 4(b)) were used to evaluate the surface morphology of pure ZnO nanoparticles and Pani/ZnO nanocomposite. The micrograph of pure ZnO exhibits that most of the particles have smooth surfaces and are crystalline with size 20–40 nm. Figure 4(b) shows the micrograph of Pani/ZnO nanocomposite which is homogeneous and uniformly distributed. These observations are different and better from the reported literature [32]. The size of nanoparticles in the nanocomposites indicates that the surface of nanoparticle has interaction with pani, which is also supported by XRD analysis.

**4.1. Thermal Analysis.** Figure 5 shows the TGA thermogram of Pani/ZnO nanocomposite. The thermogram shows two weight losses as seen in Figure 5. The first decomposition step occurs from 80°C to 130°C, incurring about 4% weight loss, corresponding to the evaporation of crystallized water. The second weight loss occurs in the temperature range from 130°C to 690°C, which may be due to the decomposition of organic moiety. We observed that Pani/ZnO nanocomposite shows 4% weight loss at 130°C and 35% weight loss at 680°C.

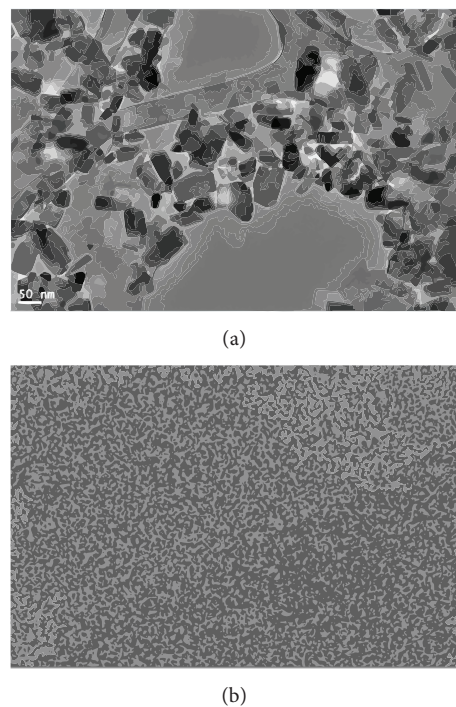


FIGURE 4: (a) HRTEM micrograph of ZnO nanoparticle and (b) HRTEM micrograph of Pani/ZnO nanocomposite.

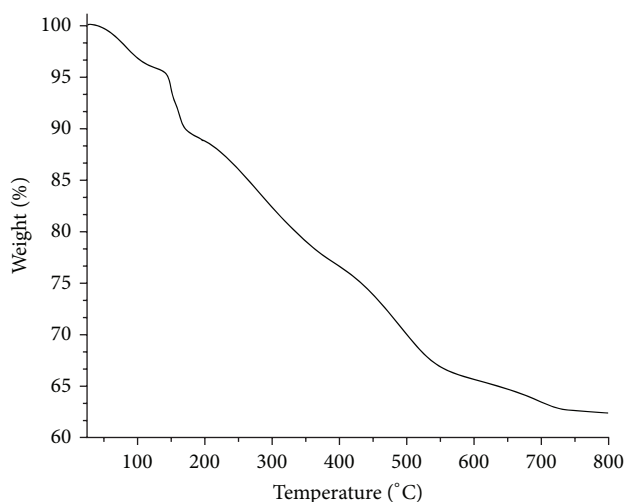


FIGURE 5: TGA thermogram of Pani/ZnO nanocomposite.

**4.2. Conductivity Studies.** The nanocomposite with 10 wt% loading of Pani in Pani/ZnO nanocomposite was prepared. The electrical conductivity of Pure Pani and Pani/ZnO nanocomposite was found to be  $3.4 \text{ Scm}^{-1}$ ,  $3.0 \times 10^{-2} \text{ Scm}^{-1}$ , respectively, when the addition of Pani in ZnO nanoparticle matrix conductivity decreases with respect to pure Pani. The change of conductivity is associated with electron transportation mechanism [30]. Pani have conjugated system easily transportation of electron, in Pani/ZnO composites create a hindrance in the path of electron and electrical

charge displaced inside the polymer, that is, decreases the conductivity.

## 5. Conclusions

Pani/ZnO nanocomposite was prepared by *in situ* polymerization of aniline using ammonium peroxodisulfate as an oxidizing agent. Synthesis of Pani was confirmed by spectroscopic techniques. Morphology of ZnO nanoparticle and Pani/ZnO nanocomposite shows uniform distribution throughout the Pani matrix investigated by HRTEM images. FT-IR and UV-Vis analysis confirm that there are strong chemical interactions between Pani and ZnO nanoparticle, which causes the red shift due to the quanta effect of ZnO and energy band between Pani and ZnO. Conductivity of Pani/ZnO nanocomposite was found to be  $3.0 \times 10^{-2} \text{ Scm}^{-1}$ . Pani/ZnO nanocomposite may find application in new electric and photoelectric devices.

## Acknowledgment

This project was supported by King Saud University, Deanship of Scientific Research, College of Science, Research Center.

## References

- [1] Y. Dong, Y. Ma, T. Zhai, Y. Zeng, H. Fu, and J. Yao, "A novel approach to the construction of core-shell gold-polyaniline nanoparticles," *Nanotechnology*, vol. 18, no. 45, Article ID 455603, 6 pages, 2007.
- [2] A. R. B. M. Yusoff and S. A. Shuib, "Metal-base transistor based on simple polyaniline electropolymerization," *Electrochimica Acta*, vol. 58, no. 1, pp. 417–421, 2011.
- [3] L. Geng, Y. Zhao, X. Huang, S. Wang, S. Zhang, and S. Wu, "Characterization and gas sensitivity study of polyaniline/SnO<sub>2</sub> hybrid material prepared by hydrothermal route," *Sensors and Actuators B*, vol. 120, no. 2, pp. 568–572, 2007.
- [4] S. Yu, M. Xi, X. Jin, K. Han, Z. Wang, and H. Zhu, "Preparation and photoelectrocatalytic properties of polyaniline-intercalated layered manganese oxide film," *Catalysis Communications*, vol. 11, no. 14, pp. 1125–1128, 2010.
- [5] C. C. Buron, B. Lakard, A. F. Monnin, V. Moutarlier, and S. Lakard, "Elaboration and characterization of polyaniline films electrodeposited on tin oxides," *Synthetic Metals*, vol. 161, no. 19–20, pp. 2162–2169, 2011.
- [6] M. Deepa, S. Ahmad, K. N. Sood, J. Alam, S. Ahmad, and A. K. Srivastava, "Electrochromic properties of polyaniline thin film nanostructures derived from solutions of ionic liquid/polyethylene glycol," *Electrochimica Acta*, vol. 52, no. 26, pp. 7453–7463, 2007.
- [7] C.-L. Zhu, S.-W. Chou, S.-F. He, W.-N. Liao, and C.-C. Chen, "Synthesis of core/shell metal oxide/polyaniline nanocomposites and hollow polyaniline capsules," *Nanotechnology*, vol. 18, no. 27, Article ID 275604, 6 pages, 2007.
- [8] S. Srivastava, S. Kumar, V. N. Singh, M. Singh, and Y. K. Vijay, "Synthesis and characterization of TiO<sub>2</sub> doped polyaniline composites for hydrogen gas sensing," *International Journal of Hydrogen Energy*, vol. 36, no. 10, pp. 6343–6355, 2011.
- [9] D. Patil, P. Patil, Y.-K. Seo, and Y. K. Hwang, "Poly(o-anisidine)-tin oxide nanocomposite: synthesis, characterization and application to humidity sensing," *Sensors and Actuators B*, vol. 148, no. 1, pp. 41–48, 2010.
- [10] M.-H. Tsai, C.-J. Chang, P.-J. Chen, and C.-J. Ko, "Preparation and characteristics of poly(amide-imide)/titania nanocomposite thin films," *Thin Solid Films*, vol. 516, no. 16, pp. 5654–5658, 2008.
- [11] X. Zhang, S. Wei, N. Haldolaarachchige et al., "Magnetoresistive conductive polyaniline-barium titanate nanocomposites with negative permittivity," *The Journal of Physical Chemistry C*, vol. 116, no. 29, pp. 15731–15740, 2012.
- [12] L.-C. Ji, L. Huang, Y. Liu et al., "Optical and electrical properties of zinc oxide/indium/zinc oxide multilayer structures," *Thin Solid Films*, vol. 519, no. 11, pp. 3789–3791, 2011.
- [13] M. Mekewi, A. Shebi, A. I. Iman, M. S. Amin, and T. Albert, "Screening the insecticidal efficacy of nano ZnO synthesized via *in-situ* polymerization of crosslinked polyacrylic acid as a template," *Journal of Materials Science & Technology*, vol. 28, no. 11, pp. 961–968, 2012.
- [14] G. Murugadoss, "Synthesis and characterization of transition metals doped ZnO nanorods," *Journal of Materials Science & Technology*, vol. 28, no. 7, pp. 587–593, 2012.
- [15] A. M. Peiró, C. Domingo, J. Peral et al., "Nanostructured zinc oxide films grown from microwave activated aqueous solutions," *Thin Solid Films*, vol. 483, no. 1–2, pp. 79–83, 2005.
- [16] M. Prach, V. Stone, and L. Proudford, "Zinc oxide nanoparticle and monocytes: impact of size, charge and solubility on activation status," *Toxicology and Applied Pharmacology*, vol. 266, no. 1, pp. 19–26, 2013.
- [17] D. Zhang, J. Zhang, Z. Guo, and X. Miao, "Optical and electrical properties of zinc oxide thin films with low resistivity via Li-N dual-acceptor doping," *Journal of Alloys and Compounds*, vol. 509, no. 20, pp. 5962–5968, 2011.
- [18] J. M. LaForge, M. T. Taschuk, and M. J. Brett, "Glancing angle deposition of crystalline zinc oxide nanorods," *Thin Solid Films*, vol. 519, no. 11, pp. 3530–3537, 2011.
- [19] P. R. Solanki, A. Kaushik, A. A. Ansari, and B. D. Malhotra, "Nanostructured zinc oxide platform for cholesterol sensor," *Applied Physics Letters*, vol. 94, no. 14, Article ID 143901, 3 pages, 2009.
- [20] P. R. Solanki, A. Kaushik, A. A. Ansari, G. Sumana, and B. D. Malhotra, "Zinc oxide-chitosan nanobiocomposite for urea sensor," *Applied Physics Letters*, vol. 93, no. 16, Article ID 163903, 3 pages, 2008.
- [21] A. A. Ansari, R. Singh, G. Sumana, and B. D. Malhotra, "Sol-gel derived nano-structured zinc oxide film for sexually transmitted disease sensor," *Analyst*, vol. 134, no. 5, pp. 997–1002, 2009.
- [22] L. Tang, X. Ding, X. Zhao, Z. Wang, and B. Zhou, "Preparation of zinc oxide particle by using layered basic zinc acetate as precursor," *Journal of Alloys and Compounds*, vol. 544, pp. 67–72, 2012.
- [23] A. A. Ansari, A. Kaushik, P. R. Solanki, and B. D. Malhotra, "Nanostructured zinc oxide platform for mycotoxin detection," *Bioelectrochemistry*, vol. 77, no. 2, pp. 75–81, 2010.
- [24] R. Khan, A. Kaushik, P. R. Solanki, A. A. Ansari, M. K. Pandey, and B. D. Malhotra, "Zinc oxide nanoparticles-chitosan composite film for cholesterol biosensor," *Analytica Chimica Acta*, vol. 616, no. 2, pp. 207–213, 2008.

- [25] M. A. Kannjwal, F. A. Sheikh, N. A. M. Barakat, X. Li, H. Y. Kim, and I. S. Chronakis, "Zinc oxide's hierarchal nanostructure and its photocatalytic properties," *Applied Surface Science*, vol. 258, no. 8, pp. 3695–3702, 2012.
- [26] T. Dentani, K.-I. Nagasaka, K. Funabiki et al., "Flexible zinc oxide solar cells sensitized by styryl dyes," *Dyes and Pigments*, vol. 77, no. 1, pp. 59–69, 2008.
- [27] J.-M. Zhang and X.-M. Feng, "Mechanistic study on electrochemical codeposition of mixed zinc-erbium oxide films on the cathodic surface," *Materials Letters*, vol. 62, no. 17-18, pp. 3224–3227, 2008.
- [28] B. Gupta, A. Jain, and R. M. Mehra, "Development and characterization of sol-gel derived Al doped ZnO/p-Si photodiode," *Journal of Materials Science & Technology*, vol. 26, no. 3, pp. 223–227, 2010.
- [29] K. G. B. Alves, J. F. Felix, E. F. de Melo, C. G. Dos Santos, C. A. S. Andrade, and C. P. de Melo, "Characterization of ZnO/polyaniline nanocomposites prepared by using surfactant solutions as polymerization media," *Journal of Applied Polymer Science*, vol. 125, no. S1, pp. E141–E147, 2012.
- [30] H. Gu, Y. Huang, X. Zhang et al., "Magnetoresistive polyaniline-magnetite nanocomposites with negative dielectrical properties," *Polymer*, vol. 53, no. 3, pp. 801–809, 2012.
- [31] X. Zhang, J. Zhu, N. Haldolaarachchige et al., "Synthetic process engineered polyaniline nanostructures with tunable morphology and physical properties," *Polymer*, vol. 53, no. 10, pp. 2109–2120, 2012.
- [32] F. Ahmed, S. Kumar, N. Arshi et al., "Preparation and characterizations of polyaniline (PANI)/ZnO nanocomposites film using solution casting method," *Thin Solid Films*, vol. 519, no. 23, pp. 8375–8378, 2011.

